

Prediction of Random-Velour Needle Punching Force Using Artificial Neural Network

Hasan Mashroteh, Mohammad Zarrebini and Darush Semnani

Abstract—Random-velour needling technology is a modified version of conventional needling process. Properties of the random-velour needled fabric are controlled by the structural alteration that occurs during random-velour needling, is due to re-orientation of fibers within the pre-consolidated fibrous assembly by special fork needles. This interaction results in creation of a dual structure, comprising base and pile layers. In this work the effect of needling parameters and fiber characteristics on force exerted on the fork needle was investigated. The effect of principal parameters on total average force " F_{rms} " exerted on individual fork needle was determined using an Artificial Neural Network (ANN) modeling and the error percentage of absolute average of predicted tests data was also calculated. Significance percentages of input parameters on " F_{rms} " was indicative of the similar influence of fiber characteristics and needling parameters on " F_{rms} ". Results manifested the importance of punch density and barbed needle penetration depth during initial consolidating needle-felting operation. Result of the neural network assessment testified that the network in general was capable of mapping input and output parameters.

Key words: Random-velour, punching force, fibrous assembly, needle, artificial neural network, modeling.

I. INTRODUCTION

RANDOM-VELOUR needled fabrics are produced by a modified needling operation on a machine depicted in Figure 1(a) known as random-velour needle loom. Moveable brush conveyor and structuring fork needles have replaced the conventional lamella bed-plate and barbed needles employed on conventional felting needle looms depicted in Figure 1(b) respectively. Figure 2 shows both types of needles.

Properties of the final velour fabric are controlled by the structural alteration that takes place during random-velour needling operation. The fork needles not only serve as the principal element in occurrence of the structural alterations, but also both transmit and influence the penetration forces that eventually have to be absorbed by the main frame of the loom [1-3]. Therefore, interaction of fork needle and fibers results in re-orientation of fibers within the initial pre-consolidated fibrous assembly which in turn leads to fundamental structural alteration in terms of creation of a dual structure comprising base and pile layers.

In the present work, a purposely designed force measuring system [4-5] has been used to measure forces exerted on the individual fork needle during random-velour needling in relation to fibrous assembly characteristics and needling parameters. All previous studies in the field of needle punching force measurement are limited to the effect of fiber and needle loom related parameters during conventional needle-felting process using barbed needles and so far no study in relation to forces experienced by fork needles has been reported.

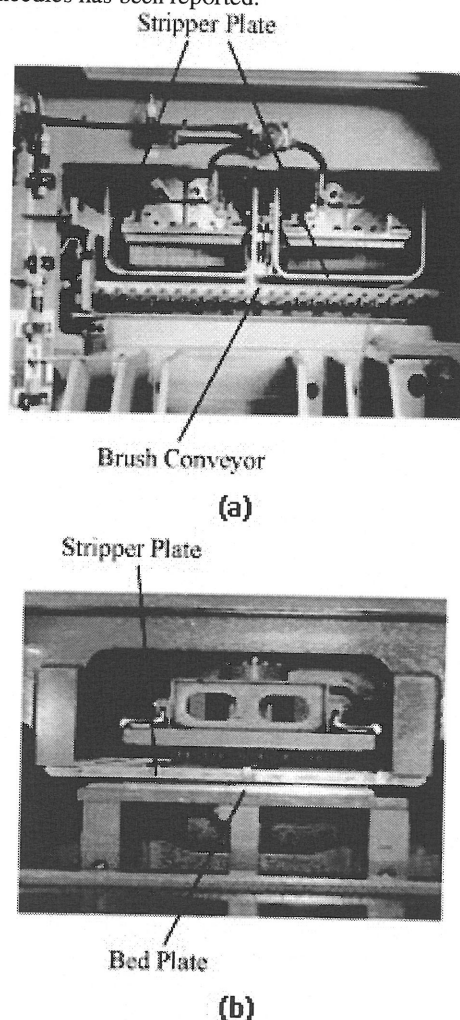


Fig. 1. Needle looms, a) random-velour loom, b) conventional felting loom.

leads to corresponding increase in magnitude of statically measured force exerted on barbed needles of a fully needled needle-board [6]. It was also reported that, in case of heavy fibrous assembly, increase in needle penetration depth results in excessive fiber breakage during needling which in turn tends to reduce the penetration force on the needle. It was confirmed that, dynamically measured punching force on single needle decreases after an initial increase as mass of fibrous assembly increases [7]. Goswami used a laboratory needle loom and reported that, fiber fineness and crimp are the pivotal factors among parameters affecting the static force experienced by the needles of a fully needled needle-board [8].

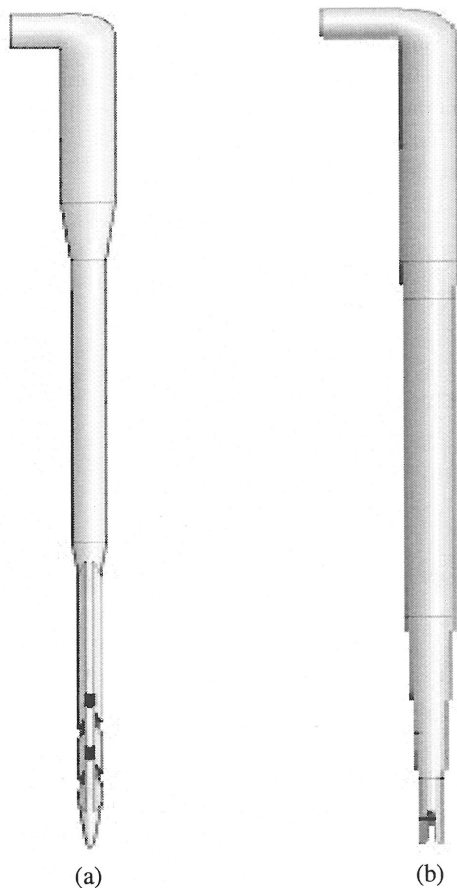


Fig. 2. Needles, a) conventional barbed needle, b) structuring fork needle.

Sarin in his 1994 review of pertained researches reported that according to Luenenschloss's studies, total forces exerted on barbed needles of a fully needled needle-board are directly proportional to stroke frequency of the needle board [9]. Seyam studies was concerned with the cumulative contributions of various factors such as needle vibration and inertia on the dynamically measured force experienced by individual barbed needle. Seyam was also successful in determining the location of the needle subjected to the highest force in relation to variation in fiber staple length and amount of punch density [10-14].

Cislo investigations showed that, quasi-static force on the barbed needle increases as both fineness and tensile strength of fiber are increased [15]. Kapusta has concluded

that, at very high needling stroke frequency, force experienced by barbed needle decreases. This was considered to be due to excessive fibre breakage and process generated heat [16]. Watanabe showed that provided both needling and fiber related parameters are held invariant, then the force exerted on the needle increases with increases in geometry of barb parameters [17].

Advances in Artificial Neural Network (ANN) have created great potential for modeling of complex engineering behaviors such as signal processing and engineering control. "ANN" has also been used in the various fields of textile researches such as prediction of pilling tendency of wool knits, seam performance of woven apparels and structural behaviors of nonwoven fabrics. Present study employs artificial neural network modeling to predict forces experienced by individual fork needle during random-velour needling.

II. ARTIFICIAL NEURAL NETWORK MODELING

An artificial neural network is a computational structure, consisting of a number of complex networks of processing elements, known as nodes, that dynamically responses to an external input. The neural network learns the governing relationships in the data set by adjusting the weights among nodes. A neural network essentially functions as a tool that maps input vectors to output vectors [18]. Figure 3 shows a fully-connected feed-forward neural network used in this study. This model comprises of an input, a hidden and an output neuron layers.

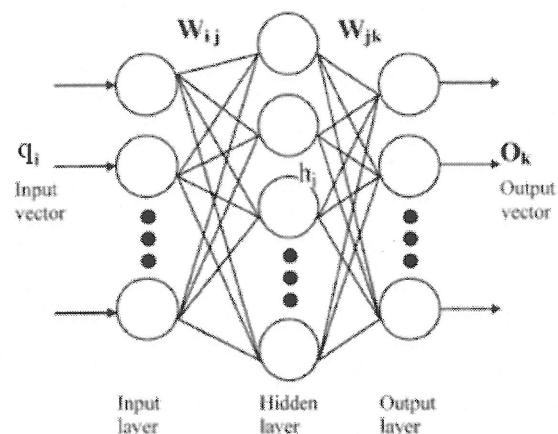


Fig. 3. A fully-connected three-layers feed-forward neural network.

The transfer functions are logistic sigmoid and linear respectively, as shown in Figure 4, where "n" and "m" are number of input parameters and number of hidden layer respectively.

The vector values of hidden-layer neurons (h_j) is calculated using continuously valued input vector q_1, q_2, \dots, q_n and a transfer function that acts in relation to W_{ij} values which are the weights between the input, hidden layers and b_j values (bias) between the input and hidden layers according to Eq. (1).

The unique desired output value (Q_k) is obtained in

terms of Eq. (2) by continuation of the Eq. (1) operations among hidden and output layers. Figure 4 depicts logistic sigmoid and linear transfer functions. "m" and "n" denote number of hidden layer and input parameters respectively.

$$h_j = f\left(\sum_{i=1}^n W_{ij}q_i - b_j\right), \quad (1)$$

where, $f(x)$ is a logistic sigmoid function, i.e.

$$f(x) = \frac{1}{1 + e^{-x}}.$$

$$O_k = g\left(\sum_{j=1}^m W_{jk}q_j - b_k\right) \quad (2)$$

k represents the number of output layer, W_{jk} are the hidden and output layers connecting weights, b_k denotes the bias connecting the hidden and output layers and g is a linear function.

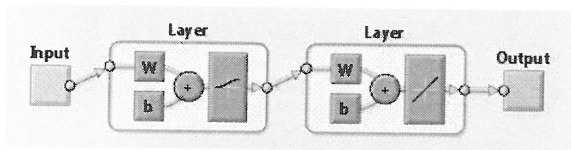


Fig. 4. Transfer functions, a) logistic sigmoid function, b) linear function.

In order to predict the total average force, an artificial neural network model based on a multi-layered feed-forward back-propagation algorithm comprises of nine inputs and one output neuron was developed. The ANN model was used to map the total average force " F_{rms} " and input parameters. Pairs of input-output were presented to the network. Weights were adjusted so that the error between the network generated output and the actual values was minimized. The output of the model formed the total average force experienced by the fork needle during random-velour needling.

III. DESIGN OF FORCE MEASUREMENT SYSTEM

Block diagram of the designed force measuring system is depicted in figure 5. The system precisely displays needling stroke frequency by incorporation of a precision Rotary Variable Differential Transformer (RVDT). Cyclic angular position of the main shaft in relation to vertical position of the needle board is also displayed.

Based on elimination principle, the twin load cell shown in figure 6 precisely measures the contribution of the factors such as vibration, inertia, frictional resistances of brush conveyor, dwell of the needle board at bottom dead center and characteristics of consolidated fibrous assembly to total force. A "BONGSHIN Miniature Load Cell", type CBFS, capacity 5 kg sensor with rated output of 1.0 mV/V was used. However, since the present study deals with the effect of fiber and needling related parameters on the total force only data acquired from one load cell is cumulatively analyzed.

Data acquisition and analysis are carried out using a purposely designed MATLAB R2010a based Force Analysis Software abbreviated to (FAS). The "FAS" capabilities include alteration of sampling start time and

inputting of calibration equation of the load cell in the software.

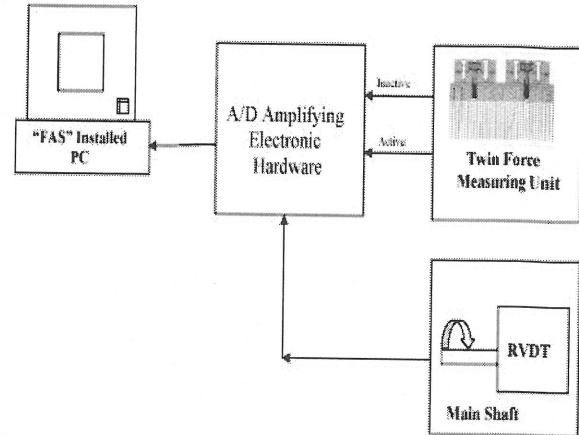


Fig. 5. Force measuring system block diagram.

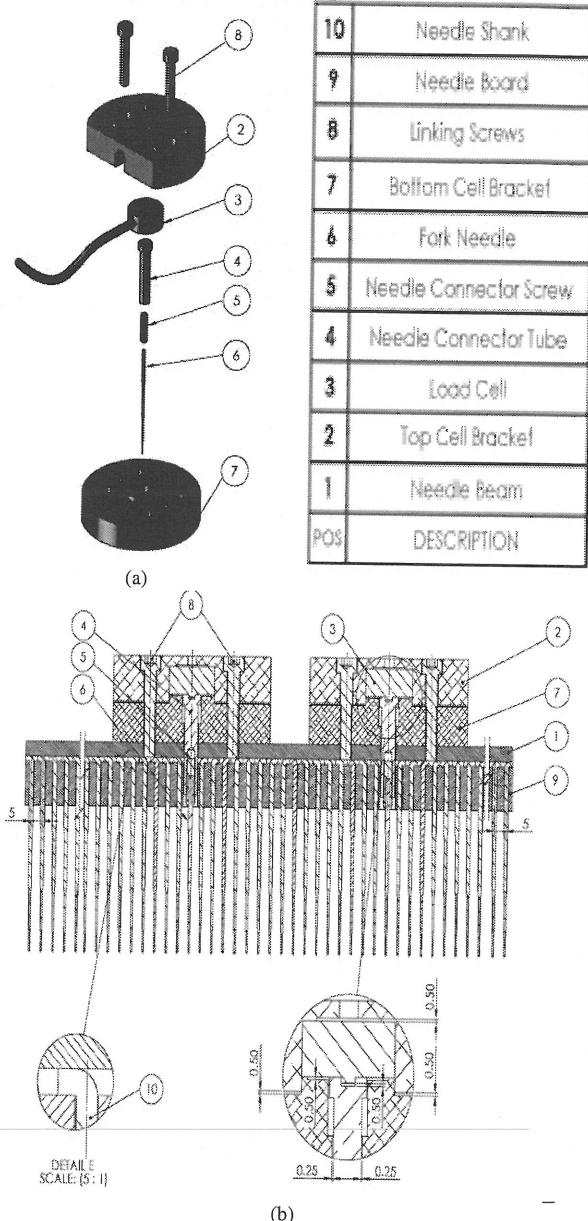


Fig. 6. Force measuring unit, a) off-machine, b) on-machine.

IV. EXPERIMENTAL

Since both needle looms and needles are designed on deflection principals therefore, quantification of force exerted on fork needles during fiber re-orientation is of vital importance. It has been also established that fiber characteristics together with needling adjustments, during both needle felting and random-velour needling operations are pivotal not only as far as physical and mechanical behavior of random-velour needled fabric is concerned, but also can probably affect the force exerted on the fork needle [19].

In this work, a total of sixty four different random-velour needled fabrics were prepared. In order to achieve the most comprehensive analysis, a large number of fiber and needling related independent variables (X_1 to X_9) as described in Table I, were defined. Variables X_1 to X_3 denote fineness, mean staple length and crimp frequency of the fiber respectively. X_4 represents mass per unit area of felted fibrous assembly. X_5 and X_6 denote barbed needle penetration depth and punch density during needle-felting operation respectively. The measured magnitudes of total average force " F_{rms} " was selected as dependent or output variable (Y) by manipulation of three independent variables X_7 , X_8 and X_9 , represent fork needle penetration depth, stroke frequency and punch density during random-velour needling respectively. Total average force represents root mean value of the squared discrete force signal of individual fork needles acquired during given stroke cycles, according to Eq. (3).

$$F_{rms} = \sqrt{\frac{\sum_{i=1}^n F_i^2}{n}} \quad (3)$$

when:

F_{rms} : Root mean value of the squared discrete force signal,

F_i : i^{th} Value of the force signal, and

n : Total numbers of force signal (at rate of 25×10^3 per second).

Magnitude of " F_{rms} " for an individual needle is in fact power of force signal for the needle. " F_{rms} " can be needle loom energy consumption index, provided " F_{rms} " encompass all fork needles then.

Carded 25 g/m² polyester web was delivered to a horizontal cross-folding unit and fiber mean staple length for each experimental sample was calculated [20]. Cross-folded batt was fed to a conventional felting needle loom, equipped with GROZ-BECKERT 15*18*32*3 R333 G1002 barbed needles. Mass per unit area of each consolidated felted fibrous assemblies was determined. The felted materials were fed to a laboratory random-velour needle loom, shown in figure 7. This loom was equipped with GROZ-BECKERT 15*17*25*38*63.5 DG1000 structuring fork needles [21].

As can be seen in Table I, variables numerically are scattered. Therefore, input and output data were

normalized in a pre-processing step. The conversion is based on the normal function provided by Matlab helping "Prestd" order in neural network toolbox of Matlab R2010a software [22-23]. Realistic prediction total average force is made by "Prestd" preprocessing the network training set by normalizing the inputs and outputs so that each have zero mean and standard deviations of 1. The pertaining data sets of 42, 14 and 8 of the samples were randomly selected for training, validation, and test sets respectively. Non occurrence of over fitting in the final result was assured using validation set. The model error can also be evaluated using the test set.

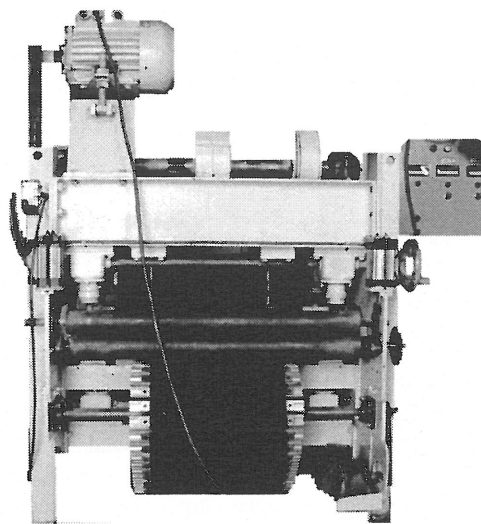


Fig. 7. Laboratory random-velour needle-loom.

The model used in this work is one hidden layered multilayer Perceptron ANN as shown in Figure 3. The hidden layer contained various numbers of neurons. Extensive training and testing of the model revealed that existence of 6 neurons in the hidden layer minimize the value of mean square error (MSE) of the model.

As shown in Figure 4, the Logistic Sigmoid function (logsig) for the first layer and the Linear function (purelin) for the last layer are used as the transfer functions. Lerenberge-Marquarte back-propagation technique was used as training algorithm of the model. This is an iterative gradient algorithm which minimizes the "MSE" value between predicted and desired output results.

V. RESULTS AND DISCUSSION

Acceptable compatibility between predicted and experimental results was achieved by minimization of error due to successive modeling trials, which led to selection of the trained model. During training, model weight and biases are varied in a manner that minimum value of model perform function are reached. By definition the perform function of the feed-forward model is mean square error (MSE) among predicted and targeted results. An ultimate MSE value of approximately 3.4×10^{-6} was obtained after performing simultaneous stages of training and validation in the 59th epoch, as shown in Figure 8.

TABLE I
MODEL VARIABLES VALUE (64 EXPERIMENTAL SAMPLES)

Sample code	Model variable									Y, F_{max} (g)
	X_1 , Fiber fineness (denier)	X_2 , Fiber length (mm)	X_3 , Fiber crimp frequency (1/Cm)	X_4 , Felted fibrous assembly mass (g/m ²)	X_5 , Punt depth, felt (mm)	X_6 , Punt density, felt (1/Cm ²)	X_7 , Punt depth, velour (mm)	X_8 , Stroke frequency, velour (s/min)	X_9 , Punt density, velour (1/Cm ²)	
1	11	121	4.5	320	7	50	8	231	100	75.44
2	11	125	4.5	321	7	50	8	463	200	97.43
3	11	128	4.5	322	7	100	8	581	300	119.69
4	11	120	4.5	335	7	125	8	696	400	121.75
5	11	129	4.5	330	9	50	10	347	200	132.51
6	11	122	4.5	333	9	75	10	233	300	108.42
7	11	129	4.5	322	9	100	10	461	100	131.77
8	11	128	4.5	334	9	125	10	579	400	151.51
9	11	126	4.5	324	11	50	12	697	300	178.92
10	11	123	4.5	332	11	75	12	463	400	150.57
11	11	124	4.5	330	11	100	12	231	100	93.30
12	11	120	4.5	318	11	125	12	582	200	147.71
13	11	128	4.5	336	13	50	12	346	400	126.92
14	11	129	4.5	319	13	75	12	462	200	136.16
15	11	120	4.5	327	13	100	14	581	100	146.71
16	11	125	4.5	329	13	125	14	695	300	173.95
17	13	90	2.3	550	7	50	8	230	100	134.13
18	13	95	2.3	540	7	75	8	462	200	148.68
19	13	87	2.3	545	7	100	8	578	300	152.34
20	13	93	2.3	548	7	125	8	691	400	164.03
21	13	92	2.3	550	9	50	10	346	200	134.50
22	13	97	2.3	554	9	75	10	231	300	120.43
23	13	93	2.3	541	9	100	10	461	100	143.90
24	13	90	2.3	549	9	125	10	693	400	164.61
25	13	85	2.3	552	11	50	12	699	300	177.92
26	13	88	2.3	564	11	75	12	462	400	147.96
27	13	92	2.3	561	11	100	12	231	100	137.47
28	13	89	2.3	538	11	125	12	585	200	165.76
29	13	96	2.3	562	13	50	12	346	400	136.33
30	13	89	2.3	547	13	75	12	463	200	149.88
31	13	91	2.3	549	13	100	14	579	100	155.58
32	13	90	2.3	559	13	125	14	695	300	208.10
33	9	124	2.7	425	7	50	8	230	100	134.42
34	9	129	2.7	420	7	75	8	462	200	143.64
35	9	127	2.7	422	7	100	8	576	300	155.45
36	9	125	2.7	430	7	125	8	695	400	166.56
37	9	126	2.7	438	9	50	10	346	200	135.74
38	9	129	2.7	440	9	75	10	233	300	129.15
39	9	127	2.7	429	9	100	10	461	100	139.28
40	9	121	2.7	438	9	125	10	579	400	196.23
41	9	120	2.7	428	11	50	12	696	300	197.91
42	9	122	2.7	441	11	75	12	462	400	189.50
43	9	124	2.7	442	11	100	12	231	100	148.51
44	9	123	2.7	434	11	125	12	581	200	169.43
45	9	125	2.7	445	13	50	12	346	400	145.33
46	9	127	2.7	427	13	75	12	462	200	153.63
47	9	126	2.7	424	13	100	14	580	100	165.08
48	9	129	2.7	430	13	125	14	695	300	192.48
49	9	71	4.0	640	7	50	8	230	100	106.10
50	9	73	4.0	650	7	75	8	462	200	133.40
51	9	75	4.0	647	7	100	8	576	300	159.57
52	9	72	4.0	652	7	125	8	695	400	162.79
53	9	74	4.0	642	9	50	10	346	200	134.55
54	9	75	4.0	652	9	75	10	233	300	124.98
55	9	76	4.0	637	9	100	10	461	100	138.11
56	9	78	4.0	647	9	125	10	579	400	191.41
57	9	79	4.0	636	11	50	12	696	300	177.82
58	9	77	4.0	645	11	75	12	462	400	184.27
59	9	75	4.0	644	11	100	12	231	100	132.41
60	9	78	4.0	637	11	125	12	581	200	184.82
61	9	76	4.0	662	13	50	12	346	400	137.82
62	9	78	4.0	641	13	75	12	462	200	145.71
63	9	79	4.0	649	13	100	14	579	100	172.16
64	9	75	4.05	650	13	125	14	695	300	183.51

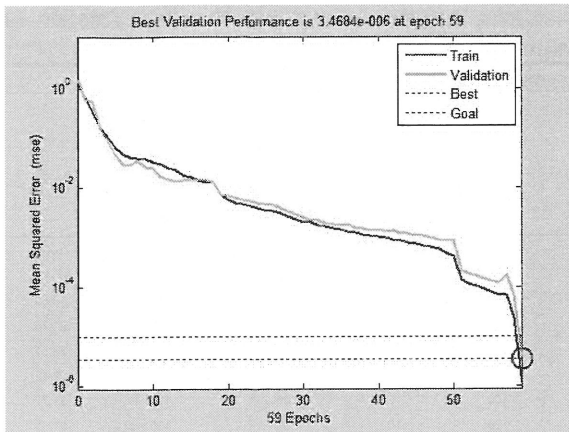


Fig. 8. Minimum Value of MSE in 59th epoch of training and validation stages.

The selected model is tested by 8 of 64 actual data. Figure 9 shows correlation values among predicted and experimental data of training ($R=1$) and test ($R=0.87589$) stages.

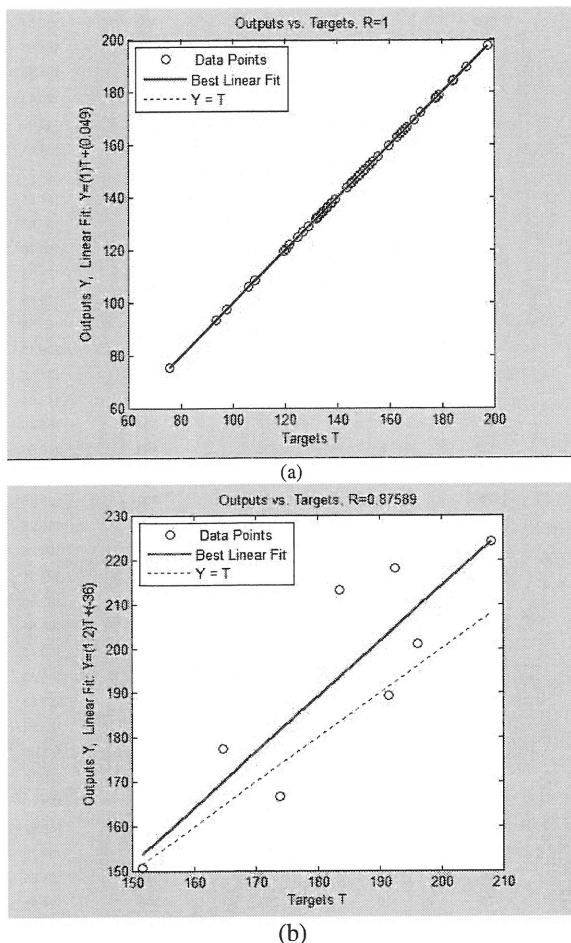


Fig. 9. Predicted and Experimental Data: a) Training, b) Test.

Training of neural network was achieved using nine input parameters. Model was tested by feeding the inputs into the network. The model generated values of total

average force " F_{rms} " were compared with experimentally obtained results. Equation 4 gives the percentage average of absolute error of eight test data.

$$\text{Error}(\%) = \frac{\sum_{i=1}^8 \left| \frac{y_i - y'_i}{y_i} \right|}{8} \times 100 \quad (4)$$

When y'_i and y_i as stated in Table II are predicted and experimental values respectively.

TABLE II
PREDICTED AND EXPERIMENTAL VALUES OF EIGHT TESTS DATA

No. of test data	Predicted value	Experimental value
	y'_i (g)	y_i (g)
1	150.5687	151.51
2	166.7048	173.95
3	177.4509	164.61
4	224.1523	208.10
5	201.1091	196.23
6	218.2833	192.48
7	189.4479	191.41
8	213.2968	183.51
Error (%) = 6.68%		

Eq. 5 [23] gives the significance percentage effect of each parameter on " F_{rms} " using neuron weights in the hidden and output layers. The results based on extraction of neurons weight in hidden and output layers from the model in relation to Tables III and IV are shown in Table V.

$$\text{Effect}_i(\%) = \frac{\sum_{j=1}^6 W_{ij}}{\sum_{i=1}^9 \sum_{j=1}^6 \sum_{k=1}^6 W_{ij} + W_{jk}} \times 100 \quad (5)$$

Table V indicates that fiber characteristics and needling parameters percentage effect more or less equally affect " F_{rms} ". Results also emphasized the importance of factors such as punch density and needle penetration depth pertaining to initial felt needling. In this regard the influence of mass per unit area of random-velour needled fabric and fiber crimp on " F_{rms} " must not be ignored.

VI. CONCLUSION

The artificial neural network has great potential for modeling of complex nonlinear textile processes. The back-propagation network model was used to predict " F_{rms} " behavior when the relative importance of inputs was known. A general model capable of predicting the combined effect of fiber characteristics, mass per unit area of initial pre-consolidated fibrous assembly together with needling adjustment during both needling stages on total average force exerted on the fork needle was developed. Validity of the model was confirmed by small value of mean square error and the relatively high coefficient of correlation of the test data. The use of validation technique

TABLE III
W_{ij} VALUES (BETWEEN INPUT AND HIDDEN LAYERS)

	W _{1j}	W _{2j}	W _{3j}	W _{4j}	W _{5j}	W _{6j}	W _{7j}	W _{8j}	W _{9j}
j=1	-10.2209	3.0422	-3.3809	-0.8074	3.3465	4.7798	-2.2070	-5.1939	-0.3095
j=2	-0.4273	-3.0007	-0.4542	-2.9269	2.6639	0.7045	-2.0218	-1.4483	0.9492
j=3	1.2983	1.2056	-4.6878	6.2337	5.4000	6.1853	-9.7229	-2.2089	-0.8152
j=4	-0.3361	0.3726	-1.2828	0.9146	-1.6754	0.3344	0.0938	-0.1564	-1.1032
j=5	1.2963	1.9592	-6.6960	5.2698	5.0740	-5.5554	1.7063	-3.5660	6.1474
j=6	-0.4100	5.4505	2.5951	3.9631	-2.8666	-5.9653	-0.1712	-1.3026	-9.2166

TABLE IV
W_{jk} VALUES (BETWEEN HIDDEN AND OUTPUT LAYERS)

	W _{1k}	W _{2k}	W _{3k}	W _{4k}	W _{5k}	W _{6k}
K=1	1.4044	-4.7716	2.4427	-3.9633	1.8466	-0.8262

TABLE V
SIGNIFICANCE PERCENTAGE OF INPUT PARAMETERS ON "F_{RMS}" VALUE

Parameters								
Fineness (denier)	Length (mm)	Crimp (1/Cm)	Mass (g/m ²)	Pent. Depth, Felt (mm)	Punch Density, Felt (1/Cm ²)	Pent. Depth, Velour (mm)	Stroke Speed, Velour (s/min)	Punch Density, Velour (1/Cm ²)
9.79%	10.15%	11.52%	11.86%	12.16%	12.99%	10.45%	9.76%	11.32%

as well as small Error% among predicted and experimental test data further verified that the ANN model is in fact the generalized mapping of the inputs and output parameters.

REFERENCES

- [1] V. Mrstina and F. Fejgl, *Needle Punching Textile Technology*. Amsterdam: Elsevier, 1990.
- [2] A. T. Purdy, *Needle-Punching*. Manchester: The Textile Institute, 1980.
- [3] T. Tyas, The design of needle looms, in *"Needle-Felted Fabrics"*, P. Lennox-Kerr, Ed. Manchester: Textile Trade Press, 1972.
- [4] H. Mashroteh and M. Zarrebini, "Analysis of Punching Force during Random-Velour Needling", *Text. Res. J.*, vol. 81, no. 5, pp. 471-481, 2010.
- [5] H. Mashroteh, M. Zarrebini and S. Ajeli, "Momentary Measurement of Force Exerted on Individual Fork Needles in Random-Velour Needling", *J. Text. I.*, vol. 104, no. 1, pp. 84-97, 2013.
- [6] J. W. S. Hearle and M. A. I. Sultan, "A study of Needled Fabrics: Part VI: The Measurement of Punching Force during Needling", *J. Text. I.*, vol. 59, no. 5, pp. 237-242, 1968.
- [7] J. W. S. Hearle and A. T. Purdy, "A Technique for the Measurement of the Punching Force during Needle-Felting", *J. Text. I.*, vol. 63, no. 7, pp. 363-374, 1972.
- [8] B. C. Goswami, T. Beck and F. L. Scardino, "Influence of Fiber Geometry on the Punching-Force Characteristics of Webs during Needle Felting", *Text. Res. J.*, vol. 42, no. 10, pp. 605-612, 1972.
- [9] S. Sarin, J. Meng and A. M. Seyam, "Mechanics of Needle Punching Process and Products: Part I: Critical Review of Previous Work on Forces Experienced by Needles during Needling of Nonwoven Fabrics", *Int. Nonwoven J.*, vol. 6, no. 2, pp. 32-36, 1994.
- [10] A. M. Seyam, J. Meng and A. Mohamed, "Mechanics of Needle Punching Process and Products: Part II: An On-Line Device to Measure the Punching Forces Experienced by Individual Needles", *Int. Nonwoven J.*, vol. 7, no. 3, pp. 31-37, 1995.
- [11] A. M. Seyam and S. Sarin, "Effect of Needle Position and Orientation on Forces Experienced by Individual Needles during Needle Punching", *Text. Res. J.*, vol. 67, no. 10, pp. 772-776, 1997.
- [12] A. M. Seyam, A. Mohamed and H. Kim, "Signal Analysis of Dynamic Forces Experienced by Individual Needles at High Speed Needle Punching", *Text. Res. J.*, vol. 68, no. 4, pp. 296-301, 1998.
- [13] A. M. Seyam, "Application of On-Line Monitoring of Dynamic Forces Experienced by Needles during Formation of Needled Fabrics", *Int. Nonwoven J.*, vol. 8, no. 5, pp. 55-60, 1999.
- [14] A. M. Seyam, "Impact of needling parameters on the locations of maximum needle force due to fiber web/ needle interaction", in *proc. Needle Punch Conference*, 2000.
- [15] R. Cislo and H. Kapusta, "Analysis of Forces Transmitted by Needles in the Process of Web Needling in Quasi-Static Conditions", *Fibres Text. East. Eur.*, vol. 10, no. 1, pp. 76-80, 2002.
- [16] H. Kapusta, "Analysis of Values of Punching Forces in the Process of Web Needling in Dynamic Conditions", *Fibres Text. East. Eur.*, vol. 11, no. 1, pp. 28-32, 2003.
- [17] A. Watanabe, M. Miwa, T. Yokoi and A. A. Merati, "Predicting the Penetrating Force and Number of Fibers Caught by a Needle Barb in Needle Punching", *Text. Res. J.*, vol. 74, no. 5, pp. 417-425, 2004.
- [18] M. B. Menhaj, *Computational Intelligence*. 3rd ed., Tehran: Amirkabir University of Technology, 2000.
- [19] H. Mashroteh, M. Zarrebini and S. Alimoradi, "Estimation of properties of random-velour polypropylene needled fabrics using multivariate regression models", in *Proc. The 4th ITC&D*, 2008.
- [20] H. Mashroteh and M. Zarrebini, "Effect of carded web weight on some properties of random-velour nonwoven floor coverings using polypropylene fibers", in *Proc. 6th Conf. Textile Engineering*, 2007.
- [21] GROZ-BECKERT, "Needles; General Catalogue", GROZ-BECKERT, Germany, 2009.
- [22] S. Haykin, *Neural Network, A Comprehensive Foundation*. New York: MacMillan 1994.
- [23] H. Demuth, M. Beale and M. Hagan, "Neural Network Toolbox User's Guide, MATLAB R2010a", The MathWorks, Inc., 1984-2010.